INTERNATIONAL JOURNAL OF
COASTAL & OFFSHORE ENGINEERING
IJCOE Vol.6/No. 4/Autumn 2021 (44-59)

Available online at http://www.ijcoe.org

Wavelet based detection of vortex shedding around a cylinder oscillating in still water

Seyede Masoome Sadaghi[1*], Seyed Taghi Omid Naeeni [2], Hasan Yousefi Ghalejoogh [3]

[1] Assistant Professor, Road, Housing & Urban Development Research Center; S.sadaghi@bhrc.ac.ir*
[2] Associate professor, School of Civil Engineering, University of Tehran, Tehran, Iran
[3] Assistant Professor, School of Civil Engineering, University of Tehran, Tehran, Iran

ARTICLE INFO

Article History:
Received: 31 Jul. 2021
Accepted: 25 Nov. 2021

Keywords:
Wavelet Analysis
Oscillatory Cylinder
Vortex Shedding

ABSTRACT

The present paper aims to study the lift forces acting on a cylinder oscillating in still water from spectral point of view. In the previous researches, vortex shedding frequency has been related to the fundamental lift frequency. Here, the wavelet analysis is used as a relatively new concept in spectral analyses. The simultaneous time-frequency representations of the lift forces are investigated to localize the flow induced transitory characteristics. The peaks in the wavelet coefficients attributed to vortex shedding are studied. The abrupt changes in the lift forces have also been studied by discrete wavelet decomposition. Small spikes have been observed in the results due to vortex shedding. Wavelet analysis is considered as an efficient alternative method to predict vortex shedding for larger Keulegan-Carpenter numbers (KC). Two different gap-to-diameter ratios, 0.1 and 1.0, are considered to account for the effect of bed proximity. Regular vortex shedding is suppressed for lower gap ratios; this fact is confirmed by wavelet analysis as well. The KC numbers in the present study are in the range of 15 to 40. The flow is in the subcritical regime with Reynolds number in the range of 9500-26000. The cylinder and the plane bed are both smooth.

1. Introduction

Submarine pipelines are very important in economical and safe transportation of oil, gas, petroleum products, fresh water and even communication cables. Generation of coherent structures in the pipe wake flow, which is generally referred to as vortex shedding, is responsible for inducing the basic excitational forces on the pipeline free spans. These forces are of great importance as they can result in the large amplitude vibrational span responses. The mechanism of vortex shedding and its influence on the flow induced forces are among the classic and important topics in fluid mechanics and have drawn attention of the researchers over the years. The growth and shedding of vortices from a submerged body (specially a pipeline) affect the velocity field and the consequent pressure on the pipeline surface. The time-varying pressure field imposes time-varying forces on the pipe surface. The velocity field around the pipe has a fluctuating pattern due to alternate vortex shedding. The frequencies of the fluctuations are highly related to the vortex shedding process. Hudgins and Kaspersen have presented and compared various conventional and wavelet-based algorithms for detecting coherent structures in wake flows.[1] Wavelet Transform (WT) is capable of providing the simultaneous time-frequency representation of signals. Most wavelet based coherent structure detection algorithms are presented for uniform flow condition and are based on velocity variations in wake flows. In this study, WT has been used for detecting vortex shedding in oscillatory flows. It has directly been applied on the lift forces to reveal the variation of frequency content in time for an average oscillation cycle.

Vortex shedding in oscillatory flows is more complicated because the near cylinder flow field has to rebuild itself twice per complete cycle as the velocity reverses direction. The cyclic acceleration of the fluid motion results in the formation of strong and usually asymmetric vortices. The flow becomes asymmetric as the vortices are swept back past the cylinder in the return half of the flow cycle. This complicated flow field affects the forces on the cylinder. WT has the advantage of revealing the peaks in the lift force traces attributed to the dominant frequency. These peaks may be attributed either to a vortex detaching from the shear layer or to a vortex washed over the cylinder in the reversal phase. Due to the simultaneous time-frequency representation of the

wavelet analysis, different sources of the peaks can be identified.

Over the years, vortex shedding process and its relation to the subsequent in-line and lift forces have been extensively investigated by force measurement and flow visualization techniques. A brief description of the achievements in this regard is presented in the following section.

2. Vortex Shedding in Oscillatory Flows

Williamson (1985) has classified vortex shedding regimes around oscillatory cylinder for different KC numbers [2]. According to the results of his studies, the number of vortex pairs being shed and convecting away from the cylinder increases with the increase in KC number. In his experiments, the force time series are obtained simultaneously with the flow visualizations. He has established a direct relation between the lift variation and the motion of vortices by using the fundamental lift frequency of his experimental data. He has concluded that the peaks in the lift force time series are attributed either to vortex shedding or to the return of the vortices towards the cylinder just after the flow reversal. The fact that a positive lift force is produced when there is a vortex moving over the cylinder was also shown by the theoretical work of Maull and Milliner (1978) [3]. Table 1 summarizes the classification of vortex shedding patterns for different KC numbers based on Williamson [2]. N_L is the normalized fundamental lift frequency by flow cycle and N is the number of vortices per half cycle.

Sumer and Fredso [4] have also investigated the vortex shedding regimes and their relation to the lift variations based on previous works by Williamson. A similar conclusion about the different vortex shedding regimes has been presented in their book.

Different modes of vortex shedding and pairing have also been introduced in the report by J. P. Kenny and partners Ltd. (1993) [5]. According to this report, at smaller KC numbers, the distances moved by fluid particles past the cylinder between the flow reversal phases are relatively small; hence fewer vortices have time to form and be shed in each half cycle. In the idealized plane oscillatory flows used in laboratory experiments such as Sarpkaya's, it has been found that for KC values in the approximate range of 5 to 15, the vortex generation, shedding and pairing patterns lock-in to the primary flow oscillation cycle. During these locked-in phases, a single vortex is shed from the cylinder in each half cycle. The consequent transverse lift force fluctuates at a frequency, f_v, equal to twice the flow oscillation frequency, f_w.

For KC numbers in the approximate range of 15 to 25, a second mode of locked-in vortex shedding and pairing has been introduced in the aforementioned report. Two vortices are shed from the cylinder in each half cycle which pair and are swept back past alternating sides of the cylinder in sequential half cycles. This generates a fluctuating transverse lift force with a dominant frequency of three times the primary flow frequency. The detailed mechanics of these two locked-in modes of vortex shedding are addressed to the studies of Grass et al. [6].

For KC numbers greater than approximately 25, it has been concluded that there is an increasing randomization and decoupling of the interaction between the shed wake vortices and the newly forming ones in the return half flow cycle. As the KC number increases, the number of vortices completely

Table 1. Vortex shedding regimes around smooth circular cylinder in oscillatory flow. Fundamental lift frequencies observed in the experiments of Williamson [2].

KC regime	KC range	Re	$N_L=f_L/f_w$	N	Lift force trace (2 cycles)
Single pair	$7<K_C<15$	$1.8\text{-}3.8\times10^3$	2	1	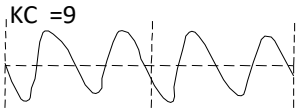
Double pair	$15<K_C<24$	$3.8\text{-}6.1\times10^3$	3	2	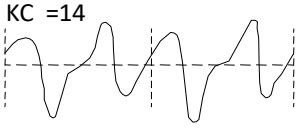
Three pair	$24<K_C<32$	$6.1\text{-}8.2\times10^3$	4	3	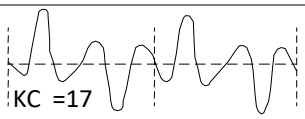
Four pair	$32<K_C<40$	$8.2\text{-}10\times10^3$	5	4	

formed and shed in each half cycle of the flow increases until the wake resembles a steady flow. According to the report by J. P. Kenny and partners Ltd., as KC number increases, the vortex shedding frequency and hence the number of complete vortices shed in each half cycle also become progressively decoupled from the primary flow oscillation frequency [5]. The number of vortices completely formed and shed in each half flow cycle, N, is directly related to the frequency of the fluctuating transverse lift force, f_v. Isaacson and Maull have suggested that f_v is given by the simple relationship $f_v=(N+1)\ f_W$ [7]. This formula is clearly valid for the two dominant vortex shedding modes discussed above for which N=1 and 2 and the lift force dominant frequencies are $2f_w$ and $3f_w$ respectively. However at larger KC values, this simple relationship can only be expected to yield approximate estimate of the overall average lift force frequency. On the other hand, the flow visualization techniques are not easily applicable for investigation of vortex shedding regimes in large KC numbers.

As stated earlier, all the peaks in the lift force time series are not induced by vortex shedding. Some peaks are associated with the return of the shed vortices towards the cylinder just after flow reversal. It is hence desirable to investigate the simultaneous time-frequency representation of the lift force traces. One drawback of using the power spectrum or frequency content of the lift force via ordinary spectral methods is that the time information of the signal is lost. It means that the ordinary spectral methods do not show when each frequency component exists in the signal. In this study, the measured forces acting on a circular cylinder oscillating in still water are used to further investigate the vortex shedding and its relation to lift force fluctuations. Wavelet analysis, which can provide the time and frequency information simultaneously, has been used to reveal the variation of frequency content in time for an average oscillation cycle.

3. Experimental Details

3.1. Experimental Apparatus

The experimental details have been fully described in the former paper by Naeeni et al [8,9]; hence only a brief description is presented here.

The experiments were carried out in the Department of Civil and Structural Engineering, University of Manchester, United Kingdom. The experimental apparatus consisted of an oscillating cylinder of 50 mm diameter kept at different gaps above a plane bed in still water. The use of air bearings in the oscillation system ensured elimination of vibrations and friction from the system interfaces thus the cylinder was free from this kind of mechanical vibrations. The motion of the oscillatory cylinder in the experiments was purely sinusoidal. The velocity of oscillation is determined according to Eq.(1). A schematic diagram of the apparatus is shown in Figure 1.

$$u(t) = U_m \cos(\omega t) \qquad (1)$$

The force transducer used in the experiments was a cantilever beam with a full arrangement of four strain gauges. The test cylinder housed the force transducer. The pressure distribution around the cylinder has also been obtained. For the pressure measurement, two pressure transducers were fixed from the inside to the wall of the cylinder in a diametrically opposite orientation. The cylinder could be rotated to locate the transducers at 36 angular positions of 10° intervals. Even though only two pressure transducers were used at a time, extreme care was taken to match the phase of the oscillations and the pressure patterns. The forces exerted on the cylinder were determined from pressure patterns as well as from direct force transducer outputs. For the same conditions of flow, forces determined from the pressure measurements are found to be in good agreement with those measured by the force transducers thus validating the measurements.

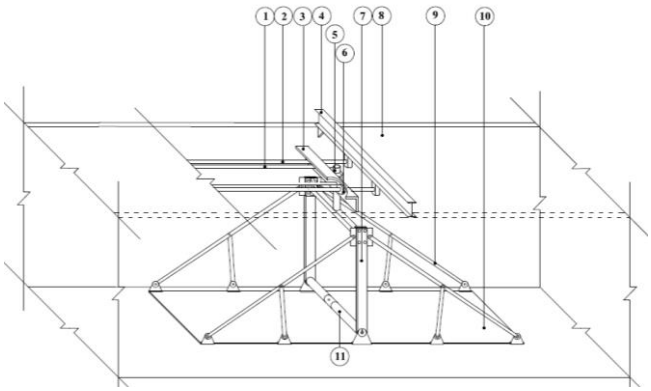

1- Connecting rods of carriage
2- Guide rods
3- Cross beams
4- Support beams
5- Swivel mount arrangement
6- Air bearing
7- Aluminum leg
8- Tank wall
9- Plate support beams
10- Plastic flat plate
11- Test cylinder

Figure 1. Experimental apparatus

3.2. Experimental Conditions

The range of test conditions for the present study is given in Table 2.

Table 2. summary of the test conditions for pressure measurements

KC	G/D	Re	β= Re/KC	U_m (m/s)	Temp (°C)	T (s)
15	0.1,1.0	9.5×10^3	630	0.19	between 17 and 23	4
20	0.1,1.0	1.3×10^4	640	0.25		
25	0.1,1.0	1.6×10^4	640	0.31		
30	0.1,1.0	1.9×10^4	640	0.38		
35	0.1,1.0	2.3×10^4	650	0.44		
40	0.1,1.0	2.6×10^4	650	0.50		

The experimental parameters in the table include the Keulegan-Carpenter number (KC), the gap ratio (G/D) which is the ratio of the gap between the cylinder and

plane bed (G) to the diameter of cylinder (D), the Reynolds number (Re), maximum velocity of the cylinder (U_m), the temperature at which the experiments were performed (Temp) and the period of oscillation (T). Each experimental run consisted of 40 cycles of oscillation of the cylinder and 256 samples were collected in each cycle.

4. Wavelet Analysis

Traditionally, turbulent statistical measures are often calculated in Fourier space. However, important temporal information is lost owing to the non-local nature of the Fourier modes and transient nature of data. Fourier Transform (FT) gives the frequency information of the signal, which means that it tells us how much of each frequency exists in the signal. However, it does not show the time when these frequency components exist. For stationary signals in which signal properties do not change over time, this drawback is not important. For non-stationary signals, transitory characteristics are often the most important part of the data series and it is important to show when these particular events took place hence FT is not suited to detect them in time domain.

Wavelet Transform (WT) can provide the time and frequency information simultaneously, hence giving a time-frequency representation of the signal. Another useful property of WT is its ability to identify abrupt discontinuities ('edges') in signals. Edges are considered as distinct variations in the smoothness or continuity. Over the past decades, the wavelet transform has emerged as a particularly powerful tool for the elucidation of fluid signals [10]. Due to their high resolution in the wavelet domain, continuous wavelets are normally employed for feature detection in flows with recognizable coherent structures. The abrupt changes in the signals or the hidden discontinuities can also be detected using wavelet decomposition.

4.1. Continuous Wavelet Transform

The continuous wavelet transform (CWT) is capable of detecting smoother signal features as well as abrupt transitions in signals in the time-frequency domain. The peaks or discontinuities in time series can be detected using this transform. The CWT uses shifted and compressed\stretched versions of a localized small wave like function to watch and measure their similarity to the data in different spatial locations. These moving functions have localized supports in both spatial and frequency domains; thereby they are known as “wavelets” or “small waves”. Stretching or compressing the wavelet corresponds to the physical notion of scale. The comparison of the signal and the wavelet at different scales and positions gives the CWT coefficients. For a scale parameter (s) and position (u), the CWT coefficient is defined as Eq.(2), (Mallet, 2009)[11]:

$$C(a,u) = \int_{-\infty}^{\infty} f(t) \frac{1}{\sqrt{a}} \psi^*(\frac{t-u}{a}) dt \qquad (2)$$

In which $f(t)$ is the signal, ψ is the mother wavelet function and * denotes the complex conjugate. This equation measures the similarity between function $f(t)$ and the window $\psi((t-u)/a)$ centered at u with scale a. The mother wavelet function is the basic form of the wavelet from which dilated and translated versions are derived and used in the wavelet transform. Multiplying each coefficient by the corresponding scaled and shifted wavelet yields the constituent wavelets of the original signal. The CWT coefficient for each position and scale represents how closely correlated the wavelet is with that section of the signal. The larger the coefficient C is in absolute value, the more the similarity. In this way the wavelet transform quantifies the local matching of the wavelet with the signal and can reveal the peaks in the lift force trace for the present study.

There are a large number of wavelets with different features which can be used for data analyses. The best one for a particular application depends on both the nature of the signal and what we desire to interrogate from the analysis. The Morlet wavelet which is believed to offer a good trade-off between detecting oscillations and peaks or discontinuities has been chosen for the present investigation. The Mother Morlet wavelet function is defined in Eq.(3) and shown in Figure 2. The C constant is used for normalization in view of reconstruction.

$$\psi(t) = Ce^{-t^2/2}\cos(5t) \qquad (3)$$

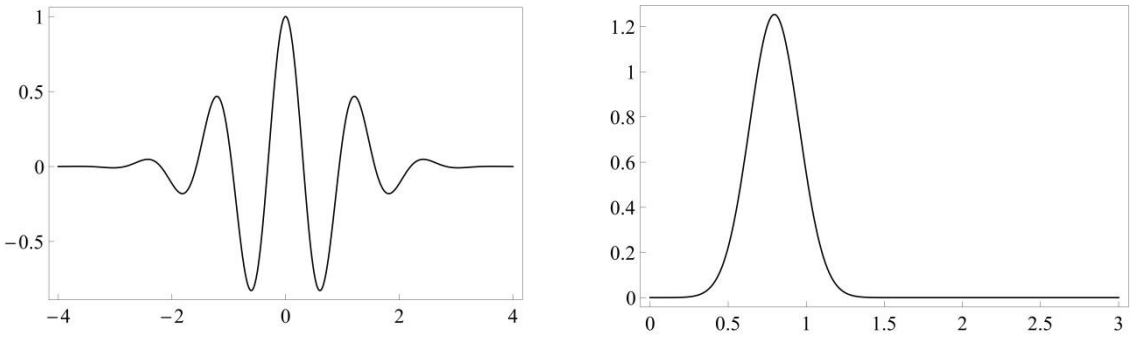

Figure 2.The mother Morlet wavelet function in time and frequency domains, (a): Time Domain, (b): Frequency Domain

In wavelet analysis, higher scales correspond to coarser signal features with lower frequencies and vice versa. While there is a general relationship between scale and frequency, no precise formula exists. As it is desired to map between a wavelet at a given scale with a specified sampling period to a frequency in Hertz, a pseudo-frequency corresponding to each scale is defined in a general sense according to Eq.(4).

$$F_a = \frac{F_c}{a.\Delta} \qquad (4)$$

In which 'a' is a scale, 'Δ' is the sampling period, 'F_c' is the center frequency maximizing the Fourier transform of the wavelet modulus in Hz and 'F_a' is the pseudo-frequency corresponding to the scale a, in Hertz.

4.2. CWT of Lift Force Variations

4.2.1. Real Wavelet Transform

The present oscillatory flow has four different phases. At the beginning of the flow cycle, the cylinder has its maximum velocity. The cylinder velocity reduces until reaching zero after a quarter of the oscillation period. Then the velocity direction reverses and the cylinder reaches its maximum velocity at the middle of the oscillation cycle. The next half of the oscillation is the same but in the reverse direction. The CWT coefficient diagram of the lift forces for KC number of 15 and two gap ratios, 1.0 and 0.1, are shown in Figure 3 as examples. The four distinct flow phases are clearly detectable in the wavelet representation of the lift force variations. The peaks in the wavelet coefficients around the dominant frequency of the lift forces, represent the vortex shedding as described earlier. The first peak occurring after the flow reversal is associated with the return of the most recently shed vortex in the previous half cycle toward the cylinder. In a half cycle between two zero velocity points ($0.25<t/T_w<0.75$), the number of vortices being shed can be found by counting the number of peaks minus one in the vicinity of the dominant frequency. As it could be seen in Figure 3, for KC number of 15 in both gap ratios, two peaks are noticeable in the wavelet scalogram. The first one which is observed just after flow reversal should be due to the return of the most recently shed vortex toward the cylinder and the second one is attributed to a new vortex being shed. Hence it indicates that for this KC number, one vortex is being shed in a half cycle for both gap ratios. This result is in accordance with previous studies for example by Williamson[2]. It is clear that the peaks could not be easily identified from the data tracing in time domain.

The CWT of lift forces on an isolated cylinder (G/D=1.0) with different KC numbers are presented in Figure 4 (a-f). The peaks in CWT coefficients around the dominant frequency of the lift forces in a half cycle are specified and the numbers of vortices being shed in each half cycle are counted accordingly.

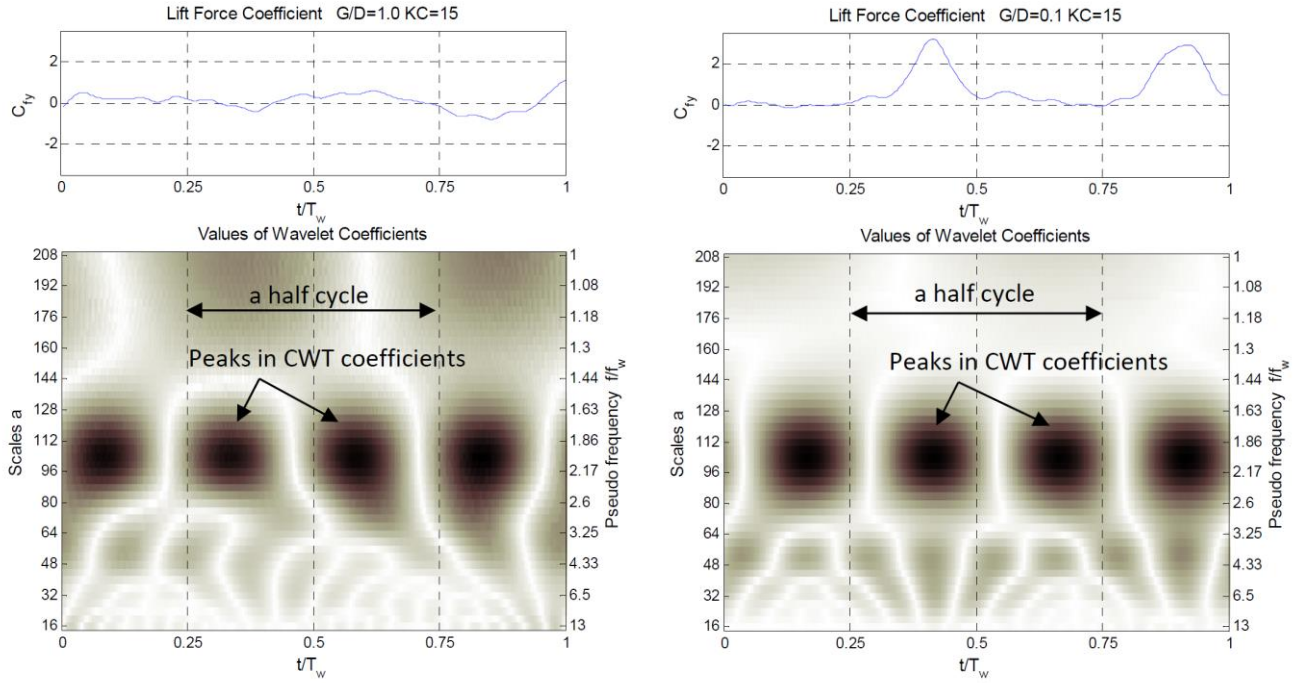

(a): G/D=1.0 (b): G/D=0.1

Figure 3. Four flow phases in the CWT diagram of the lift forces for KC number of 15 and two gap ratios of 1.0 and 0.1 , extremum values of CWT coefficients in black and zero values in white

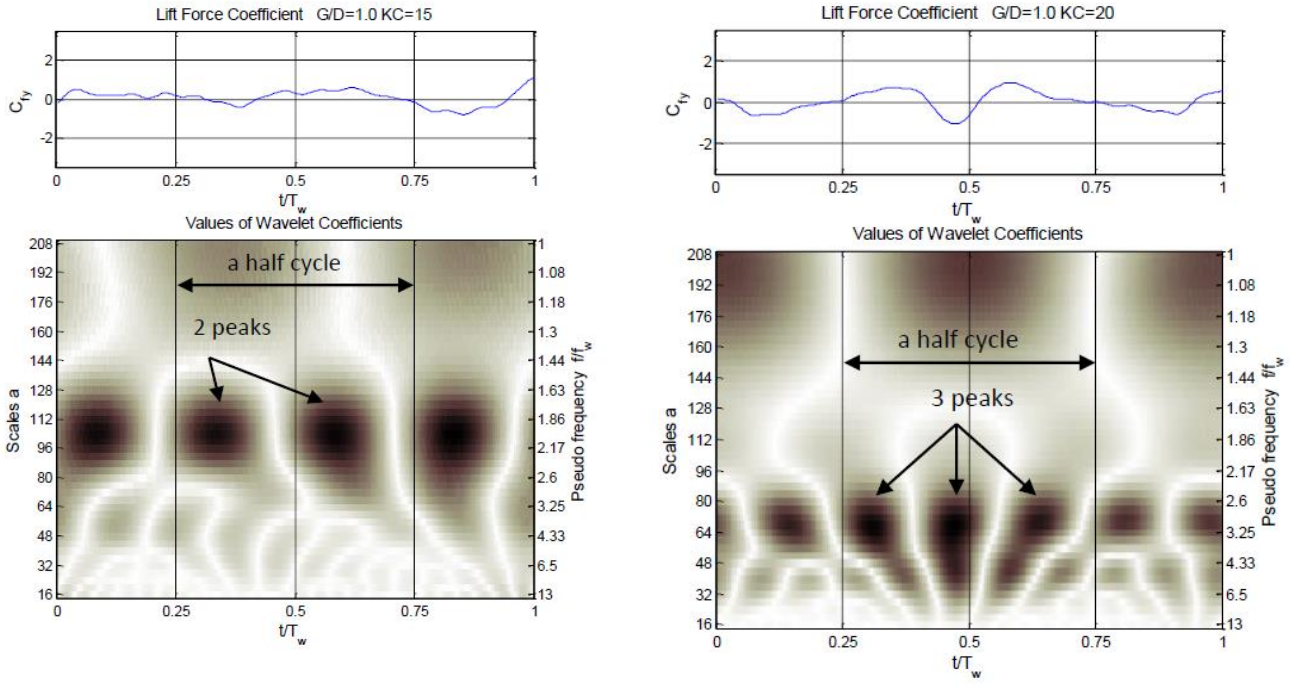

(a): KC=15 (b): KC=20

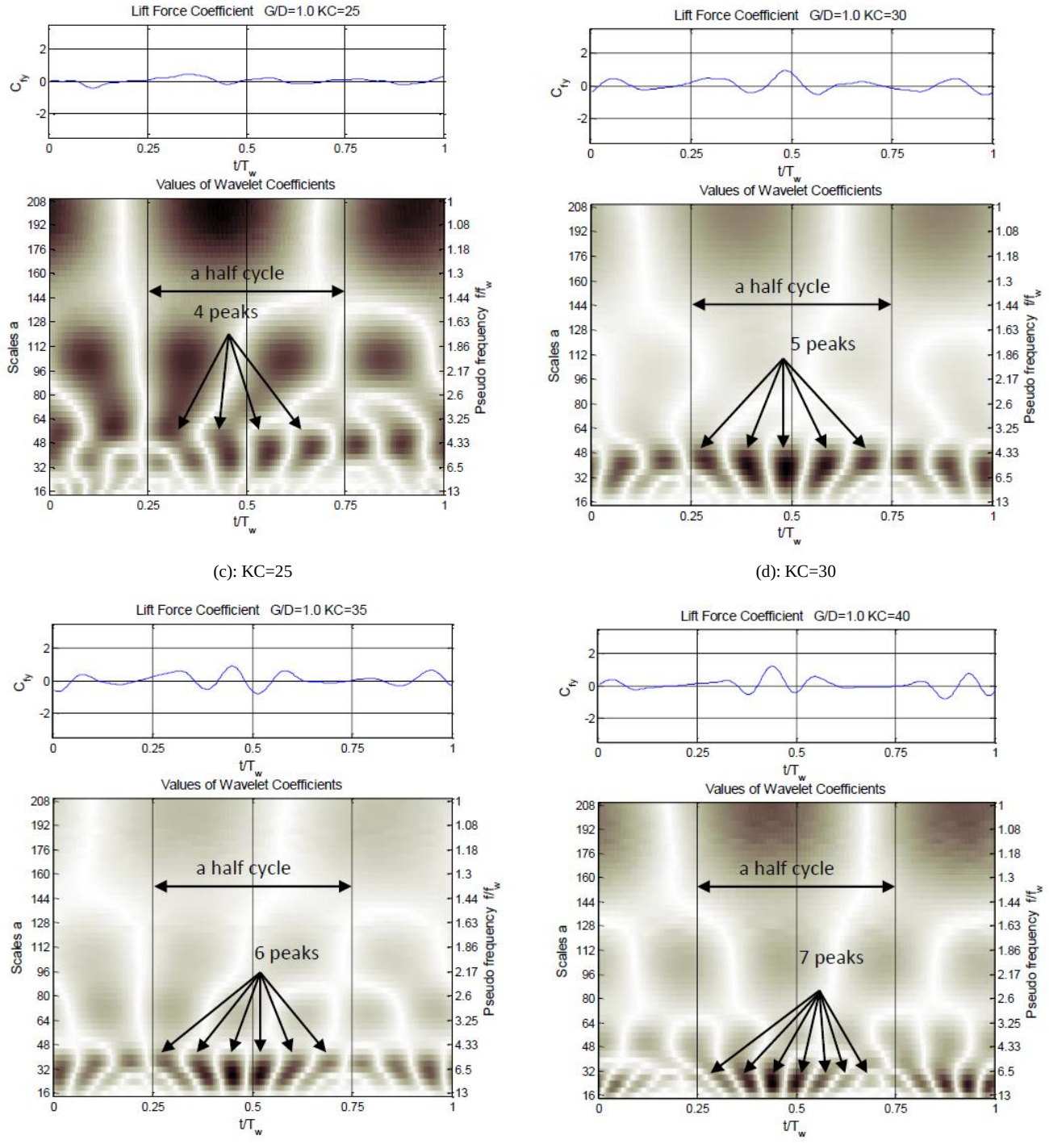

(c): KC=25 (d): KC=30

(e): KC=35 (f): KC=40

Figure 4. The CWT coefficients of lift force for different KC numbers and G/D=1.0, extremum values in black and zero values in white

As can be seen in Figure 4, the maximum CWT coefficients for KC number of 15, are detected at the relative frequency around two ($f/f_w \approx 2$). It shows that for this KC number, the dominant frequency of the lift force measurements is twice the frequency of the main oscillation. This result is due to the existence of two similar half cycles hence the velocity field contributes to the second harmonic of the lift variations. The second harmonic in the lift forces is observed for almost all studied KC numbers but it is clearly seen that the contribution of higher harmonics in the lift force variations increases for larger KC numbers. Every time a vortex is detached from the cylinder, a sudden change in form of a peak is expected in the lift force trend and consequently in the CWT coefficients. It is important to consider the peaks in CWT coefficients around the dominant frequency.

4.2.2. Complex Wavelet Transform

For further accuracy, we have also investigated the complex Morlet wavelet by which the amplitude and phase components of the signal could be separated. The amplitude component of the complex wavelet clearly shows the dominant frequency and its region. The real part which is often used to detect sharp signal

transitions is then used to count the number of peaks associated with the dominant frequency. The number of vortices being shed in each half cycle is estimated accordingly. The imaginary part of the transform detects the local extremums in the first derivatives which measures the speed of variations in data; here it can be used to detect the speed of lift force variations due to vortex shedding.

A complex Morlet wavelet is defined by Eq.(5) [10].

$$\psi(t) = \pi^{-1/4}(e^{i2\pi f_0 t} - e^{-(2\pi f_0)^2/2})e^{-t^2/2} \quad (5)$$

Where f_0 is the central frequency of the mother wavelet. The second term in the brackets is known as the correction term, as it corrects for the non-zero mean of the complex sinusoid of the first term. In practice it becomes negligible for values of $f_0 >> 0$ and can be ignored, in which case, the Morlet wavelet can be written in a simpler form of Eq.(6), [10].

$$\psi(t) = \frac{1}{\pi^{1/4}} e^{i2\pi f_0 t} e^{-t^2/2} \quad (6)$$

This wavelet is a complex wave within a Gaussian envelope. The complex sinusoidal waveform is contained in the term $e^{i2\pi f_0 t}$ $(=\cos(2\pi f_0 t)+i\sin(2\pi f_0 t))$.

The Gaussian envelope $e^{-t^2/2}$ has unit standard deviation and confines the complex sinusoidal waveform. The central frequency has been considered equal to unity for the present study. The real and imaginary sinusoids of the Morlet wavelet differ in phase by a quarter period (Figure 5). The $\pi^{1/4}$ term is a normalization factor which ensures that the wavelet has unit energy[10]. As it can be seen in Figure 5, the real part of ψ is symmetric which detects local extremums in data and the imaginary part is anti-symmetric which captures extremums in first derivative of the data.

The complex Morlet wavelet coefficient is composed of the real and imaginary parts hence we can write it in terms of its phase angle and modulus as defined in Eq.(7) and Eq.(8) respectively.

$$\varphi(s,u) = \tan^{-1}[\mathrm{Im}(C(s,u))/\mathrm{Re}(C(s,u))] \quad (7)$$

$$|C(s,u)| = \sqrt{[\mathrm{Im}(C(s,u))]^2 + [\mathrm{Re}(C(s,u))]^2} \quad (8)$$

The imaginary part is phase-shifted by one quarter of a cycle from the real part. As we use the complex conjugate in the transform, the imaginary part is inverted and lags behinds by one quarter of a cycle from the real part. The phase angle varies cyclically between $-\pi$ and π over the duration of the component waveforms. Zero phase corresponds to the real part of the Morlet wavelet centered at the maximum amplitude of the sinusoidal waveforms. A phase of π (and $-\pi$) corresponds to the minima of the real transform plot.

As examples, the results of the complex Morlet wavelet transform for KC number of 15 and 20 are shown in Figure 6 and Figure 7 respectively. For KC=15, the modulus of coefficients shows the dominant frequency of 2 hence in the graph of real parts of coefficients, the peaks around the mentioned frequency should be chosen. As it could be seen in Figure 6, in the graph for the real parts of wavelet coefficients around the dominant frequency, two peaks (one positive and one negative) are detectable. The second one is related to the vortex shedding. The graph for the imaginary parts detects the peak values of the first derivatives which are indicative of local minimum lift forces in absolute values. For KC number of 20, the dominant frequency is around 3 and there are 3 peaks in the real part of coefficients in a half cycle for the mentioned frequency (Figure 7).

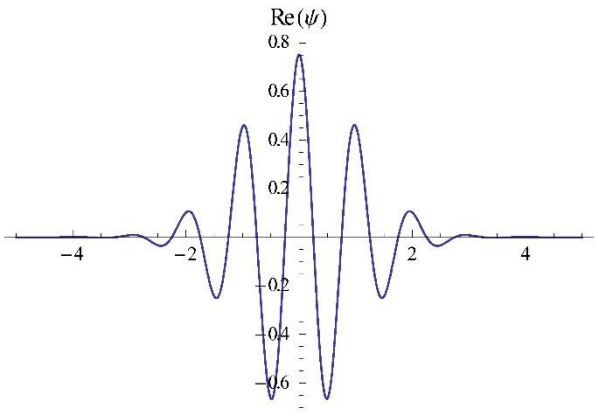

(a): Real part

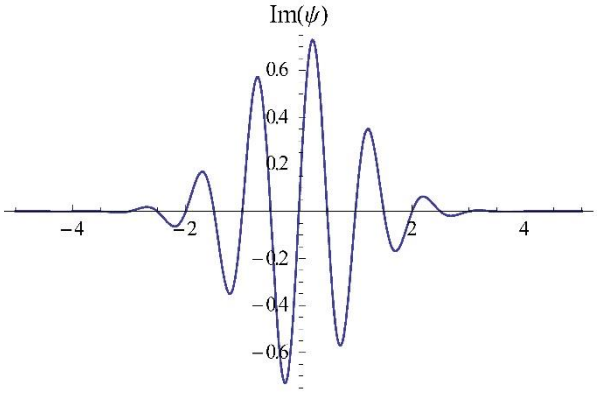

(a): Imaginary part

Figure 5. The real and imaginary parts of complex Morlet wavelet (f_0=1)

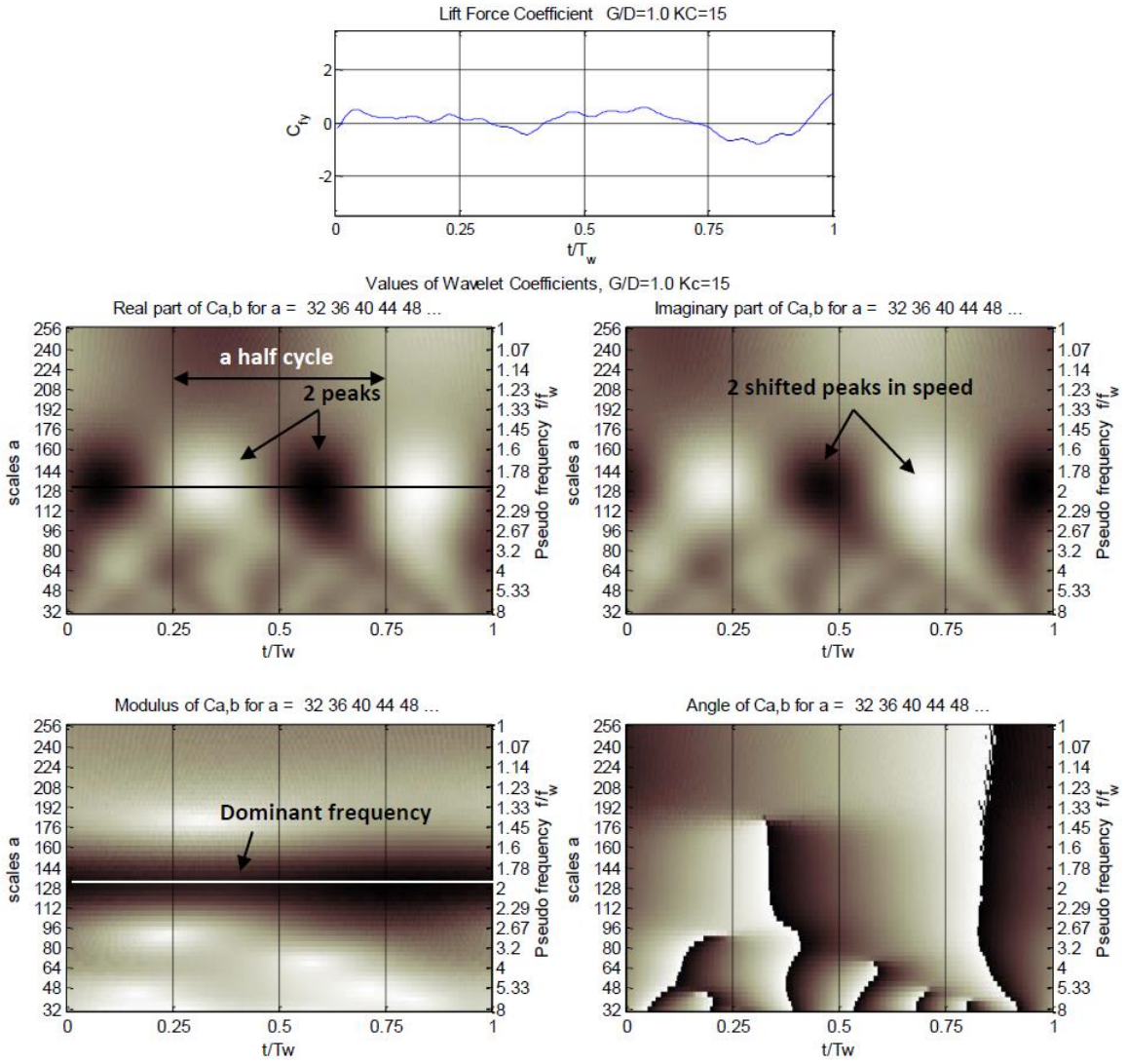

Figure 6 The complex Morlet coefficients for lift force, G/D=1.0, KC=15 (raw signal at the top followed by the different parts of the wavelet transform as specified in subplots)

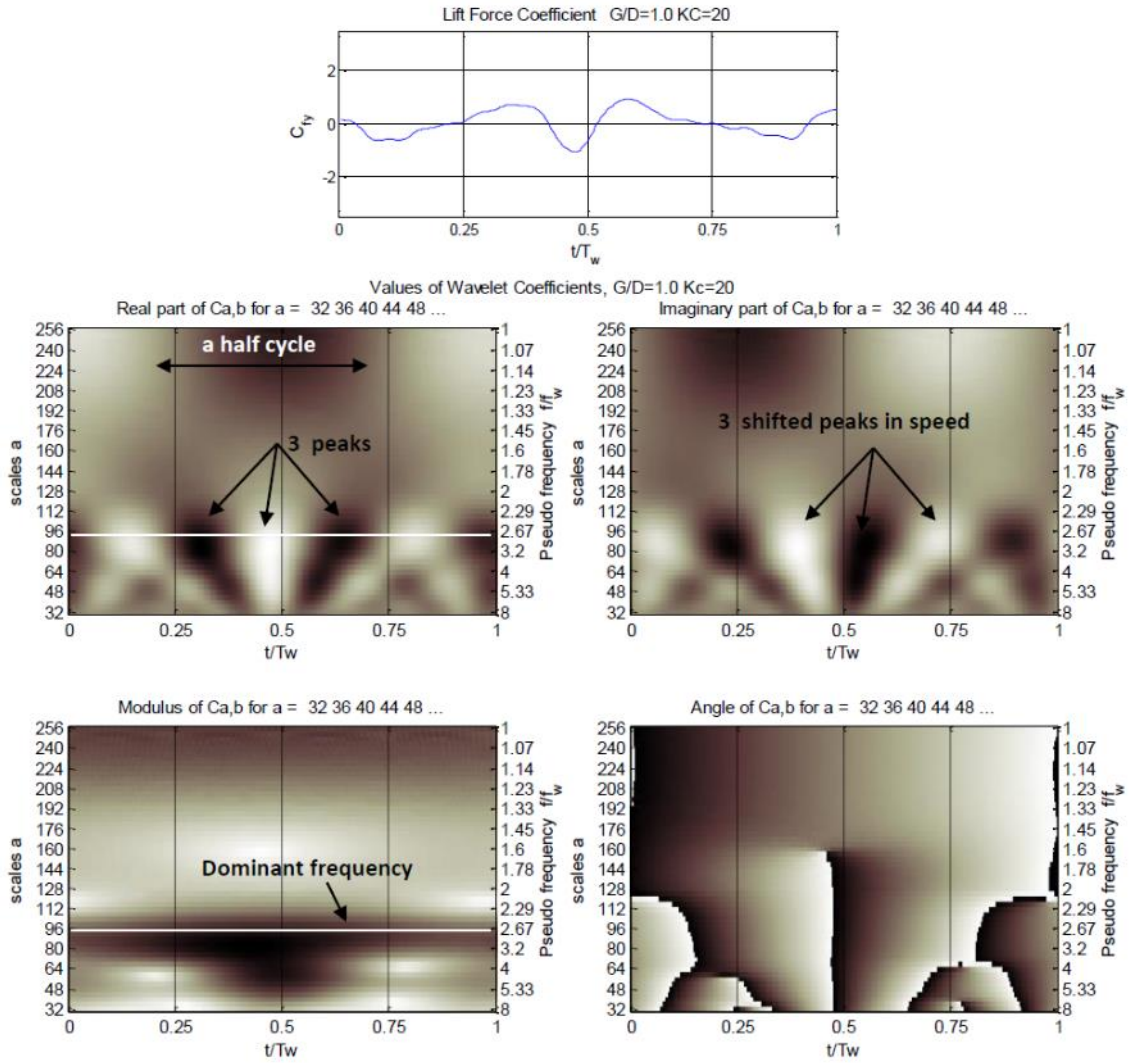

Figure 7 The complex Morlet coefficients for lift force, G/D=1.0, KC=20; (raw signal at the top followed by the different parts of the wavelet transform as specified in subplots)

The approximated numbers of vortex shedding in different KC numbers are compared with those estimated by previous works (see section 2) in Table 3. The results show that the former studies estimated less vortex shedding in a half cycle for larger KC numbers. As reported in former studies[5], for larger values of KC number, there is an increasing randomization in the formation and shedding of the vortices and flow visualization techniques are hardly applicable to trace the vortices. In fact visual tracing in higher flow velocities and consequently larger KC numbers, can lead to faulty and unreliable results. The wavelet analysis which is capable of representing the signal in simultaneous time/frequency domains could be considered as an alternative method to predict the vortex shedding in different flow conditions especially for larger KC numbers.

Table 3 Vortex shedding regimes around smooth circular cylinder in oscillatory flow.

KC range in former studies	**N_1=** Vortices per half cycle concluded from former studies	**KC number in present study**	**N_2=** Vortices per half cycle concluded from present study
7<KC<15	1	15	1
15<KC<24	2	20	2
24<KC<32	3	25	3
		30	4
32<KC<40	4	35	5
		40	6

N1=Vortices per half cycle concluded from former studies, N2=Vortices per half cycle according to the present study.

4.3. Discrete Wavelet Decomposition

As stated earlier, wavelet analysis can identify abrupt changes in the signal. Signals with very rapid evolutions such as transient signals in dynamic systems may undergo abrupt changes such as a jump or a sharp change in the first or second derivatives.

These features can be detected by wavelet decomposition. In this method, the signal is written in the form of an orthogonal sum of a rough approximation and an infinite number of finer details as shown in Eq.(9), [11].

$$f(x)=\sum_{l=0}^{2^{J_{\min}}} c_{J_{\min},l}\cdot\varphi_{J_{\min},l}(x)+\sum_{j=J_{\min}}^{J_{\max}-1}\sum_{n=0}^{2^j} d_{j,n}\cdot\psi_{j,n}(x) \qquad (9)$$

here $\varphi(x)$ and $\psi(x)$ are the scaling and wavelet functions and $\varphi_{j,k}(x)$ and $\psi_{j,k}(x)$ are the dilated and shifted versions of $\varphi(x)$ and $\psi(x)$, respectively. In cases of non-interpolating wavelets, they are: $\varphi_{j,k}(x)=\sqrt{2^j}\varphi(2^j x-k)$, $\psi_{j,k}(x)=\sqrt{2^j}\psi(2^j x-k)$. $c_{j,k}$ and $d_{j,k}$ are approximation and detail coefficients which can be obtained by the projection method using the orthogonal or bi-orthogonal feature of the wavelet family.

4.4. Discontinuity Detection

Considering wavelet transform, there are two methods to detect discontinuity in a signal namely the continuous wavelet transform (CWT) and the discrete wavelet transform (DWT). In the following examples, the application of these two methods in the detection of discontinuities in signals will be presented. The simplest form of a rupture in a signal is a step function which is investigated by CWT and DWT methods. The results are presented in Figure 8 (a-b) which show the ability of both methods to detect the rupture at time t=0.5.

The following example illustrates how the wavelet decomposition with DWT detects hidden singularities, for example, a jump in the second derivative of a signal[12]. Figure 9 shows the smooth-looking function f(t) defined by Eq.(10) and its continuous wavelet transform. As it can be seen, the CWT analysis of the signal does not show the localized singularity.

$$f(t)=\begin{cases}\dfrac{t^3}{6}, & 0\le t<0.5\\ \dfrac{t^3}{6}-\dfrac{t^2}{2}+\dfrac{t}{2}-\dfrac{1}{8}, & 0.5\le t<1.\end{cases} \qquad (10)$$

The Daubechies-3 wavelet decomposition for this function is presented in Figure 10 in which a_9 is the coarsest level approximation of the signal (s) and d_1 to d_9 are finest to coarsest details. The coarsest approximation shows an average or "trend" of the signal where d_1 with its higher frequencies in the wavelet series would show abrupt changes and discontinuities. As it can be seen in Figure 10, the discontinuity in the second derivative of the function f(t) is detected with a very good resolution as sharp spikes at t = 0.5.

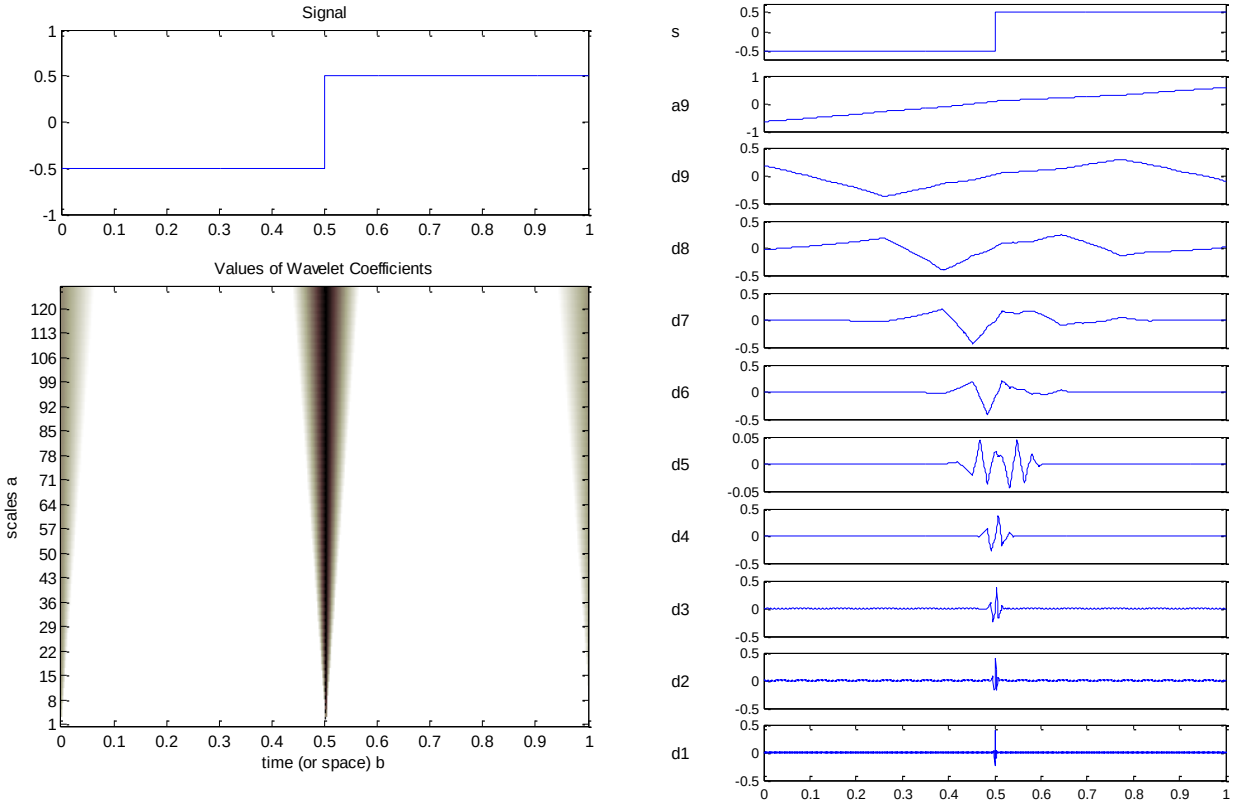

(a): CWT (b): DWT

Figure 8 The continuous and discrete wavelet transform of a step function

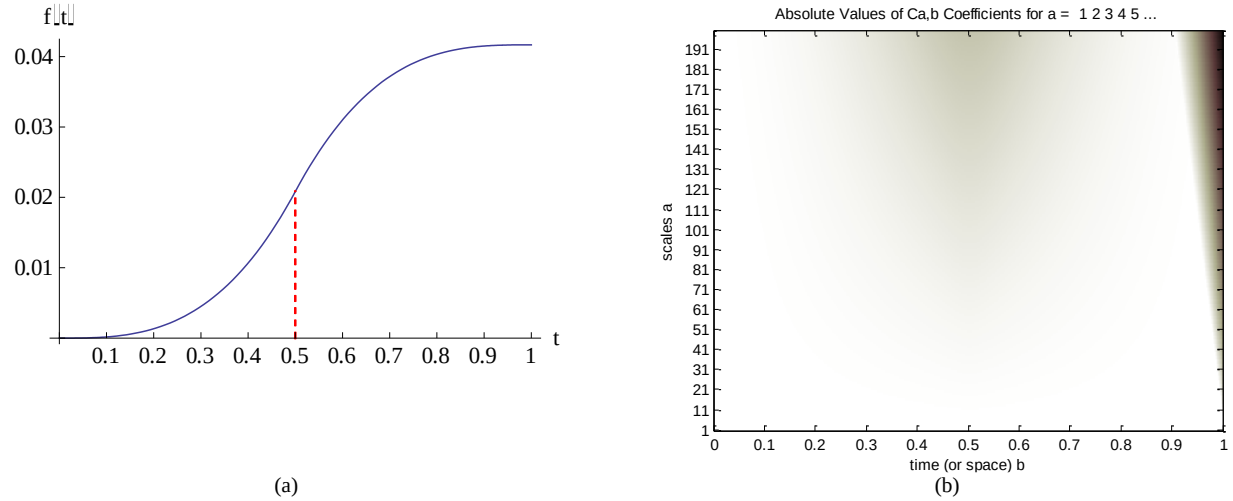

(a) (b)

Figure 9 The smooth-looking function f(t) defined by Equation (10) (a) and the corresponding CWT (b)

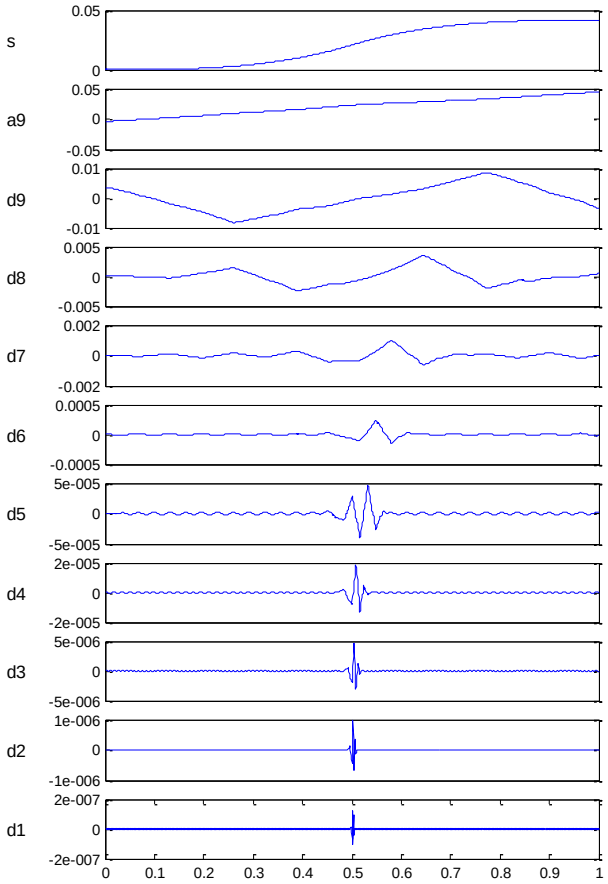

Figure 10. The Daubechies-3 wavelet decomposition for the function in Eq.(10)

The sudden changes in the lift forces attributed to vortex shedding can be detected by both CWT & DWT wavelet transforms. The inherent discontinuity can be captured by DWT; hence, DWT can be used as a robust tool to capture both sudden and inherent changes in data. For this purpose, the lift force traces for three cycles of oscillations are decomposed with Daubechies-2 wavelet. The results pertaining to KC numbers of 20 and 40 are typically presented in Figure 11.

The discontinuities between three cycles are clearly recognizable in the finest detail level (D_1) by large amplitude spikes in frequency space. Moreover, small noise like spikes can be seen in each cycle which are the consequence of changes in the lift force due to vortex shedding; however it is clear that there are no inherent sudden changes in data. The comparison of results for different KC numbers shows that these spikes are more bolded for larger KC values. The reason is that in larger KC numbers, the distances moved by the fluid particles past the cylinder between the flow reversal phases are relatively long and the vortices have more time to completely form, grow and be shed in each half cycle. For the case of KC=40, six successive spike groups can be clearly detected in each half cycle as shown in the close-up illustration of first level detail (D_1) in **Error! Reference source not found.**. This result is in accordance with the estimations from the CWT analysis. For smaller KC numbers, estimation of the vortex shedding number is not so straightforward but the discontinuities are still noticeable. Hence, this method is more suitable for flow conditions with larger KC values for which conventional methods based on flow visualization or Fourier based spectral analyses could not accurately estimate the vortex shedding frequency.

4.5. Effect of Bed Proximity on Vortex Shedding

Various studies have shown that regular vortex shedding is suppressed for lower gap ratios namely for G/D<0.3 (Naeeni and Narayanan, 2003)[13]. The wavelet analyses clearly confirm these results. The CWT coefficients of lift forces for a near bed cylinder with gap ratio of 0.1 and different KC numbers are presented in Figure 13(a-f).

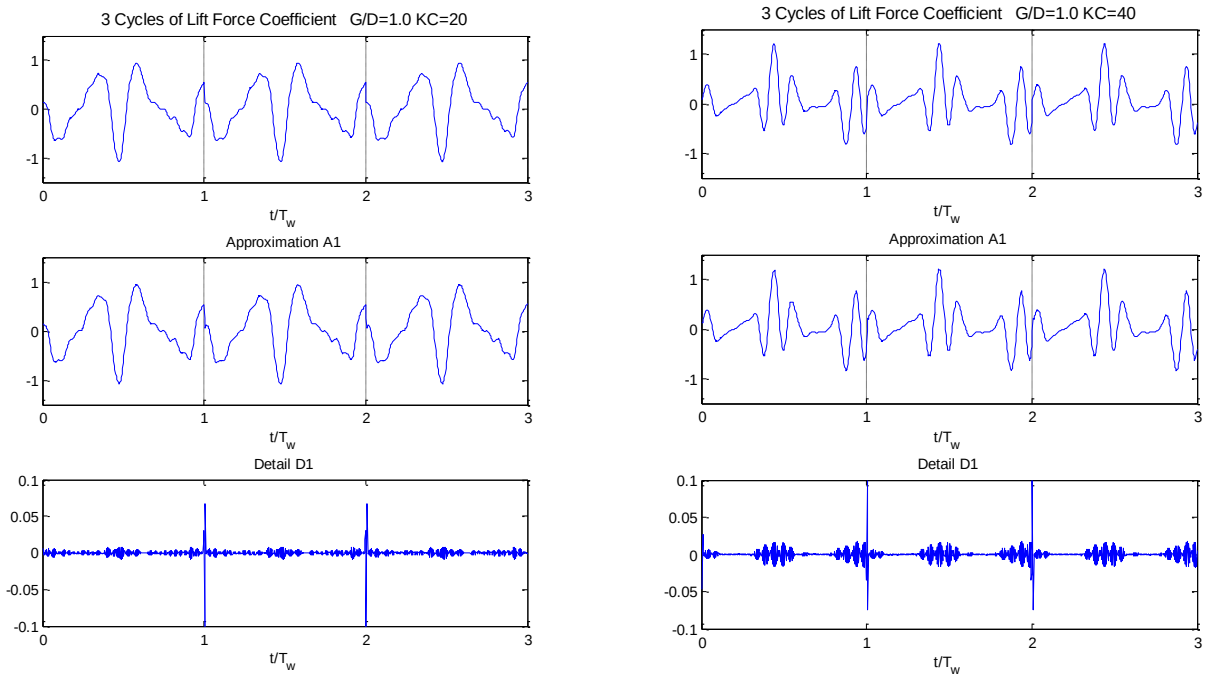

(a) (b)

Figure 11. The Daubechies-2 wavelet decomposition of lift forces, G/D=1.0, (a)KC=20, (b)KC=40

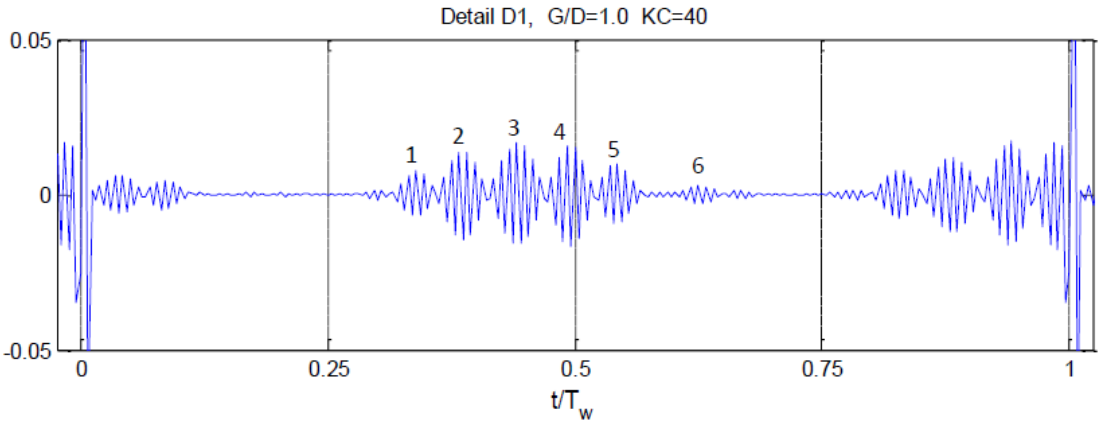

Figure 12. Close-up illustration of first level detail (D_1) of lift forces in a single oscillation cycle(G/D=1.0, KC=40), six spike groups in a half cycle indicate the number of vortex shedding

The results show that the dominant frequency of the lift force measurements for a near bed cylinder remains twice the frequency of oscillation of the cylinder for all studied KC numbers which is due to the existence of two similar half cycles in the flow regime. The flow field is divided to four distinct phases as explained in section 4-2. The higher frequency contents in lift forces which are believed to be the consequence of vortex shedding and are observed for the case of isolated cylinders are not present for the case of near bed cylinders. For a closer look, the lift force traces and their corresponding CWT coefficient scalograms for KC number of 40 and gap ratios of 1.0 and 0.1 are compared in Figure 14. The effect of vortex shedding on the creation of higher harmonics are clearly seen for the case of an isolated cylinder (G/D=1.0). These effects do not exist in the scalogram related to the near bed cylinder confirming the suppression of regular vortex shedding.

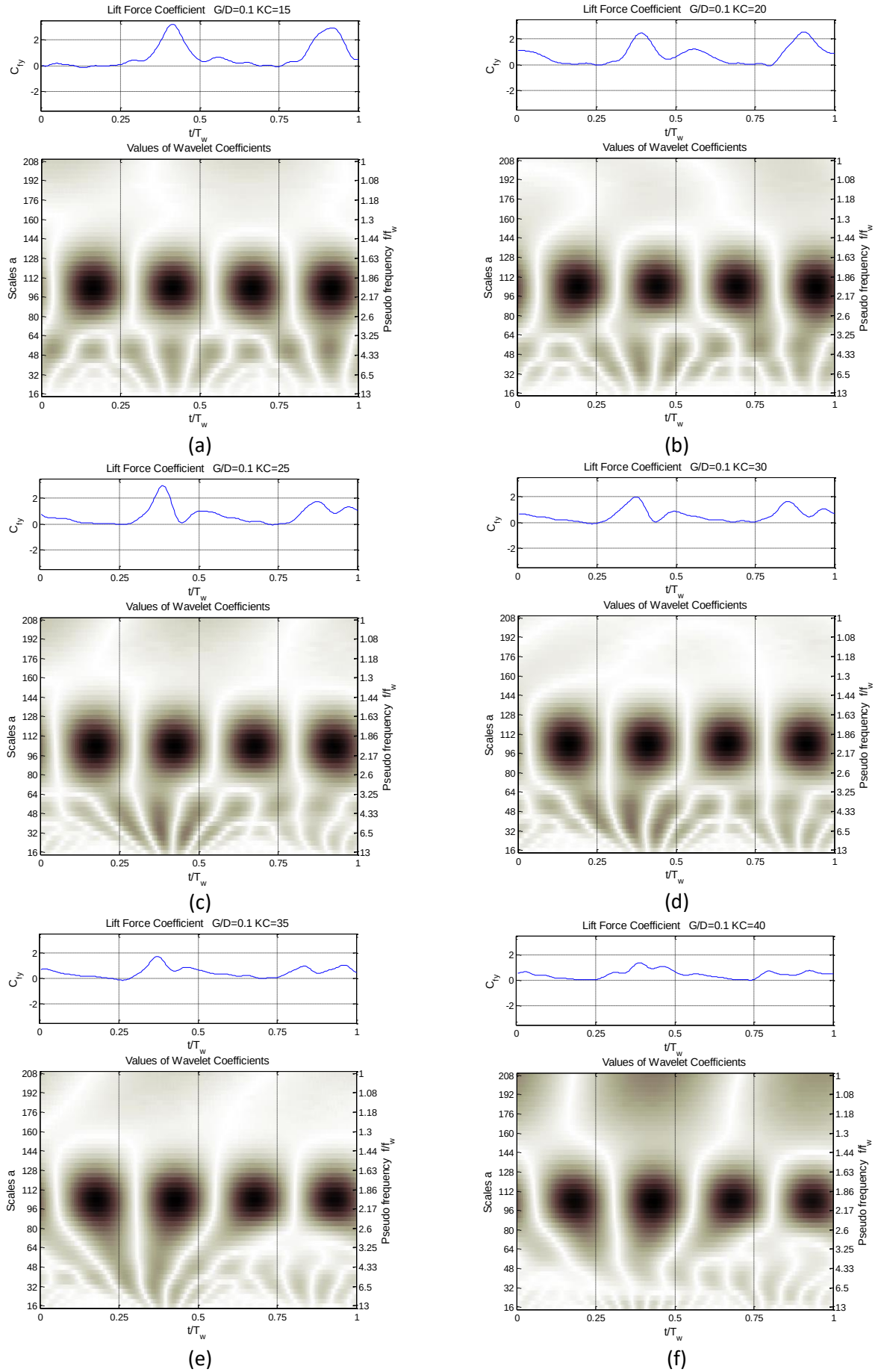

Figure 13. The CWT coefficients of lift force for different KC numbers and G/D=0.1, extremum values in black and zero values in white

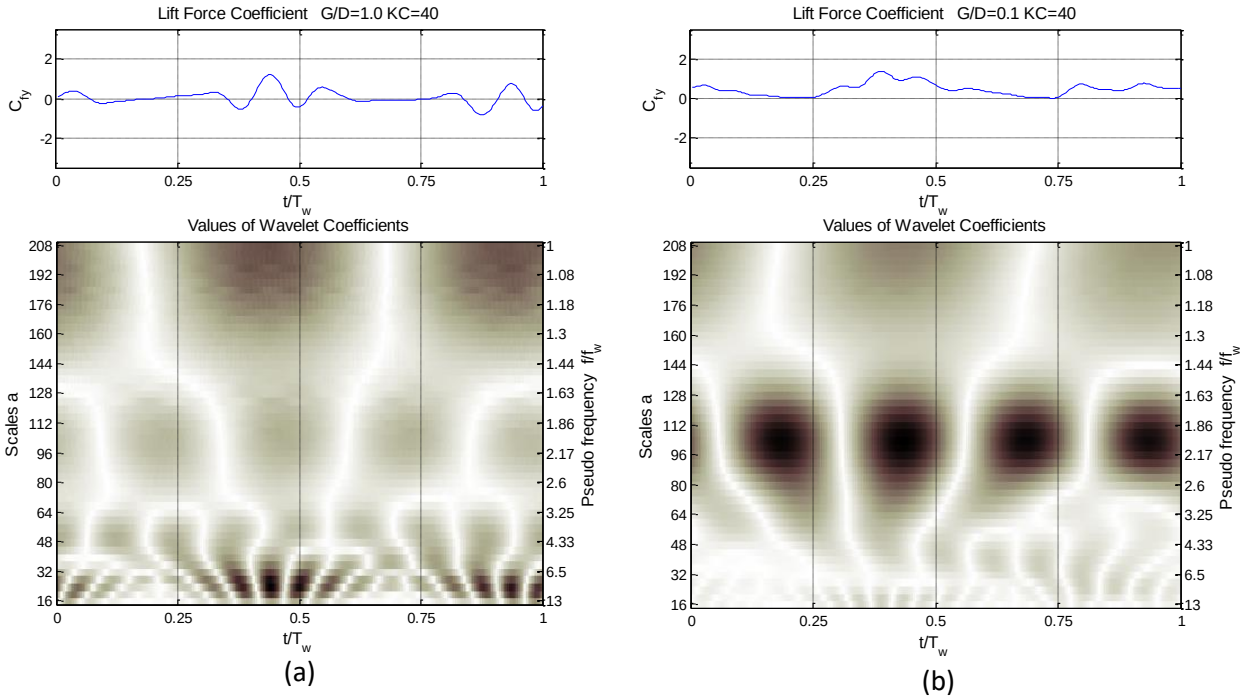

Figure 14. The CWT coefficients of lift force for KC number of 40 and two gap ratios of G/D=1.0 (a) and G/D=0.1 (b), extremum values in black and zero values in white

5. Conclusion

Wavelet analysis is an efficient method for feature detection in flows with recognizable coherent structures due to its high resolution nature. So far, most wavelet based coherent structure detection algorithms are presented for uniform flow condition and are based on velocity variations in wake flows. In the present study, wavelet analysis has been used to reveal the variation of lift force frequency content in time for an average oscillation cycle of an oscillatory flow. The four distinct oscillatory flow phases are clearly detectable in the wavelet representation of the lift force variations. Every time a vortex is detached from the cylinder, a sudden change in form of a peak is expected in the lift force trend. The symmetrical Morlet wavelet can reveal these peaks in a simultaneous time-frequency domain. The first peak in the CWT coefficient is related to the return of the most recently shed vortex in the previous half cycle. The rest of the peaks are attributed to the vortex shedding. The number of vortices shed in each half cycle is counted accordingly. This is conceivable due to the simultaneous time-frequency representation of lift force variations by wavelet analysis. Since for larger values of KC number, the randomization in the formation and shedding of the vortices increase and flow visualization techniques are hardly applicable to accurately estimate the vortex shedding frequency, the wavelet analysis is proved to be an efficient alternative method to predict the vortex shedding in different flow conditions. The wavelet analyses show more vortex shedding in a half cycle for larger KC numbers in comparison with the estimations of former studies. The discrete wavelet decomposition of the lift force time series also reveals the abrupt changes attributed to vortex shedding in the finest detail level. The discontinuities are more distinguishable for larger KC numbers. It is concluded that the method is more suitable for flow conditions with larger KC values for which conventional methods based on flow visualization or Fourier based spectral analyses could not accurately estimate the vortex shedding frequency. The fact that the regular vortex shedding is suppressed for lower gap ratios is also investigated by wavelet analysis. The results for the gap ratio of 0.1 show that the higher frequencies which are believed to be the consequence of vortex shedding and are observed for the case of isolated cylinders are not present for near bed cylinders. The dominant frequency of the lift force for a near bed cylinder remains twice the frequency of oscillation of the cylinder for all studied KC numbers which is due to the existence of two similar half cycles in the flow regime.

Acknowledgement

The authors would like to thank Dr. Rangaswami Narayanan, a former reader at the department of civil and structural engineering, University of Manchester for his assistance in experiments and also his invaluable technical supports that greatly improved the manuscript.

References

[1] Hudgins, L., Kaspersen, J.H., (2004). Wavelets and detection of coherent structures in fluid turbulence, Wavelets in Physics, Edited by J.C. Van Den Berg, Cambridge University Press, UK, 201-226.

[2] 2.Williamson, C. H. K., (1985). Sinusoidal Flow Relative to Circular Cylinders. J. Fluid Mech., 155, 141-174.
[3] Maull, D. J., Milliner, M. G., (1978). Sinusoidal Flow Past a Circular Cylinder, Coast. Eng., 2, 149-168.
[4] 4.Sumer, B.M. and Fredsoe, J., (2006). Hydrodynamics around Cylindrical Structures, Advanced Series on Ocean Engineering - Volume 26, World Scientific Publishing Co., Singapore.
[5] Kenny, J. P. and partners Ltd., (1993). Evaluation of Vortex Shedding Frequency and Dynamic Span Response, Development of Guidelines for Assessment of Submarine Pipeline Spans, Background Document One, OTI93614, Published by Health and Safety Executive.
[6] Grass, A. J., Kemp, P.H., Stuart, R. J., (1981). Vortex Induced Velocity Magnification and Loading Effects for Cylinders in Oscillatory Flow. SERC London Centre for Marine Technology. Report Number FL 28 January.
[7] Isaacson, M., Maull, D. J., (1976). Transverse forces in vertical cylinders in waves, J. Waterw. Port Coast. Ocean Eng., Div. ASCE WWI.
[8] Naeeni, S.T.O., Sadaghi, S.M., Narayanan, R., (2013). Effect of bed proximity on the in-line forces acting on a cylinder oscillating in still water, Ocean Eng.
[9] Naeeni, S.T.O., Sadaghi, S.M., Narayanan, R., (2015). Spectral Features of the Pressure Distribution Around a Cylinder Oscillating in Still Water, Coastal Engineering Journal, Vol. 57, No. 3
[10] Addison, P. S., (2002), The Illustrated Wavelet Transform Handbook, Introductory Theory and Applications in Science, Engineering, Medicine and Finance. Institute of Physics Publishing, Bristol and Philadelphia.
[11] Mallat, S., (2009). A Wavelet Tour of Signal Processing, Elsevier Inc., United States.
[12] Jerri, A.J., (2011). Introduction to Wavelets, Sampling Publishing, Potsdam, New York.
[13] Naeeni, S.T.O., (2003). Force on Yawed Circular Cylinder Oscillating over a Plane Bed in Current, PhD thesis, UMIST, Manchester, UK.